

SYNTHESIS AND CHARACTERIZATION STUDY OF MANGANESE DIOXIDE NANOMATERIAL USING SIMPLE CHEMICAL PRECIPITATIVE METHOD

¹Priyadharshni K ²Anandhi Sarangapani

Department of physics
Faculty of Arts & Science
Bharath Institute of Higher Education and Research
Chennai India -600 073

[¹Kdharshnimsc@gmail.com](mailto:Kdharshnimsc@gmail.com) [²Ananthi.Physics@bharathuniv.ac.in](mailto:Ananthi.Physics@bharathuniv.ac.in)

Address for Correspondence

¹Priyadharshni K ²Anandhi Sarangapani

Department of physics
Faculty of Arts & Science
Bharath Institute of Higher Education and Research
Chennai India -600 073

[¹Kdharshnimsc@gmail.com](mailto:Kdharshnimsc@gmail.com) [²Ananthi.Physics@bharathuniv.ac.in](mailto:Ananthi.Physics@bharathuniv.ac.in)

Abstract

At presently, manganese oxide nanoparticles (MnO₂ NPs) have intrigued material science researches XRD widely owing to its extensive variety of applications. In this study, the manganese oxide nanoparticles were prepared by using manganese chloride Tetra hydrates salts. The samples were characterized to find the structural, functional and magnetic properties by XRD, FT-IR, and VSM respectively. An attempt is made to summarize the complete field dependent magnetization study of the synthesized material is presented. Structural studies by XRD indicate that the synthesized material as tetragonal crystal structure. FT-IR analysis revealed stretching vibrations of metal ions in tetrahedral and octahedral co-ordination confirming the crystal structure. The Antiferro magnetic behaviour was observed at room temperature with no saturation magnetization and hysteresis in the region of measured field strength. These measurements as a function of temperature and field strength showed a reduction in Anferromagnetic temperature.

Keywords: *Nanoparticles; Manganese oxide; Metal oxide; Transition metal oxide, FTIR, VSM*

Introduction

Materials at the nanoscale have recently taken up a lot of attention among researchers due to the unique characteristics of physical and chemical compared to the bulk counterparts. Although the

nanometer scale is typically represented as 1-100 nm, nanoscience and nanotechnology frequently deal with things larger than 100 nm nanomaterial.. Metal oxide nanostructures have recently received a lot of interest because of their potential use as functional components for nano-electronics, optoelectronics, and sensing devices with an electronic structure. They may be metallic, semiconducting, or insulating in nature. Oxides can also be utilised to create a circuits of microelectronics, sensors, piezoelectric devices, fuel cells, corrosion-resistant surface coatings, and other devices.. Many important applications for metal oxides namely as iron, nickel, cobalt, manganese, copper and zinc have been studied, having magnetic storage media, solarenergy transformation, electronics, semiconductors and catalysis [**Vijayamari .,2016**]. These materials exhibit unusual optical and electrical characteristics as a result of a phenomena known as Quantum Confinement. Common metal oxide nanocrystals, namely MnO, MgO, CaO, ZnO, TiO₂, and Al₂O₃ have been proven to be very effective and active absorbers of a wide range of hazardous substances, as well as air pollutants, chemical warfare weapons, and acidic gases. Because of its Superparamagnetic properties, metal oxides such as Fe₂O₃, BaFe₁₂O₁₉ are utilised in cancer diagnosis and treatment, sensors, and memory systems. [Foster, 2006] and [Hasan Bagheri, 2020]. Manganese exists in a number of oxidation states as well as chemical and structural forms. Because of their strong reducing potential, manganese oxides are also aggressive oxidants. Only a combination of different manganese oxides (MnO₂, Mn₂O₃, and Mn₃O₄) is generally produced due to the diversity of oxidation states and the rapid phase transitions of MnO_x during production. Moreover, manganese oxyhydroxides (MnOOH) are often related phases in wet synthesis. Manganese oxide refers to any of several manganese oxides and hydroxides [Wells, 1987]. Manganese oxides are one of the most common minerals on the world, and they may be found in a wide range of natural sediments, soils, and ores. They're also in desert rock varnish and marine manganese oxides [Achurra2009]. There are many naturally occurring crystalline manganese oxides with close MnO₂ stoichiometry, as well as several amorphous manganese oxides [Achurra2009, Luo 2008, Nitta1984, and Cao 2010.,]. Furthermore, crystalline material architectures are mostly composed of edge-shared MnO₆ octahedral units that are organised to resemble tunnelled or layered structures. MnO contributes to the high porosity and surface areas of the material's structure..

These MnO nanoparticles are significant due to their distinct characteristics, which include a high surface-to-volume ratio, high crystallinity, chemical purity, and phase selectivity when compared

to their bulk equivalent. It has been observed that the physical and chemical characteristics of a substance are related to its stoichiometry, particle size, and shape. MnO₂, Mn₃O₄ nanoparticles have the potential to be utilised in a variety of applications, including electrodes [Lind1988], catalysis [Xi, 2004], sensors [Li., 1997], and optoelectronics [Shchukin., 2007].

Section snippets

Chemicals

All chemicals used were of analytical grade and were commercially obtained. Manganese Chloride hexahydrate [Mn(Cl₂)₂.6H₂O], the precursor for Manganese, Sodium hydroxide (NaOH), the oxide source, Ethanol, Deionized Water were purchased from E-Merck, India. Because the chemicals were of analytical reagent grade with 99 percent purity, they were utilised exactly as received.

Synthesis of Manganese Oxide NPs .

At room temperature, a manganese oxide nanoparticle was created through a simple chemical precipitative procedure. In this study, a synthesis process for 0.2M MnCl₂ was thoroughly documented. In 100 ml of distilled water containing 0.44 g of NaOH aqueous solution, 4H₂O was dissolved. With continual stirring, 25 mg of trisodium citrate was added as a surfactant, which can prevent nanoparticle reunion. After 24 hours of stirring, a brown colour precipitate was produced, indicating that the reaction had completed. The precipitate produced is filtered, cleaned several times through Deionised water as well as ethanol with dried overnight in a hot air oven at about 80 °C. The surfactant Trisodium citrate was removed by calcining the as-prepared sample at 500 °C for four hours below air at a ramping rate of 5°C min⁻¹.



Fig 3.1 photo image of typical Mn-O₂ precipitation after the reduction process

. The samples were then examined using X-ray diffractometer (XRD) using Cu-K₁ radiation in the 2θ range of 20° – 90°, FTIR in the area 400 – 4000 cm⁻¹, and Vibrational Sample Magnetometer .

RESULTS AND DISCUSSIONS

XRD - pattern of manganese oxide nanopowder

As shown in Fig.3.1, the XRD pattern is utilised to identify the phase and purity of the produced MnO₂ nanoparticles. The diffraction peak locations are acquired using an XRD diffract metre at the values of 18.1°, 29°, 32.4°, 36.2°, and 60°, which correspond to the crystal planes (101), (112), (103), (211), and (224), respectively. In view of the distinctive diffraction peaks are properly indexed to and agree with the previously reported tetragonal structure of MnO₂ single phase (JCPDS card no. 24-0734). (Vazques-olmos 2005, America.)

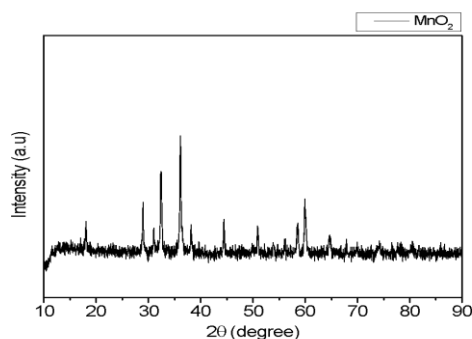


Fig.3.2 : XRD pattern of the annealed under 500 degree C for 3 hours manganese dioxide nanocrystal powder

Analysis of Functional group Using FTIR

Fig.3.2 depicts the FT-IR spectrum of produced Mn₃O₄ nanoparticles. The bands detected at 400–750 cm⁻¹ give information on the octahedral structure of MnO₆, whereas the bands observed at 3500–750 cm⁻¹ indicate the vibration caused by Mn interaction with OH, O, H, and C groups. Mn–O stretching modes occur at higher wavenumbers, whereas Mn–O bending vibrations occur at lower wavenumbers. The Mn–O stretching modes of Tetrahedral and Octahedral units may be ascribed to the distinctive vibrational mode of two wide absorption peaks situated at 473.51 cm⁻¹ and 596.12 cm⁻¹. The vibrational mode at 473.51 cm⁻¹ is caused by bending vibration, whereas the vibrational mode at 596.01 cm⁻¹ is caused by stretching vibrations of Mn–O bonds in MnO₆ octahedral. The presence of hydroxyl stretching vibrations causes the high absorption peak at 3410 cm⁻¹. The weak absorption peak found around 1629 cm⁻¹ refers to moisture adsorption on the plane of the sample, whereas a tiny

peak at 1372 cm⁻¹ belongs to OH bending vibrations coupled with Mn atoms represented (Table 3.1)

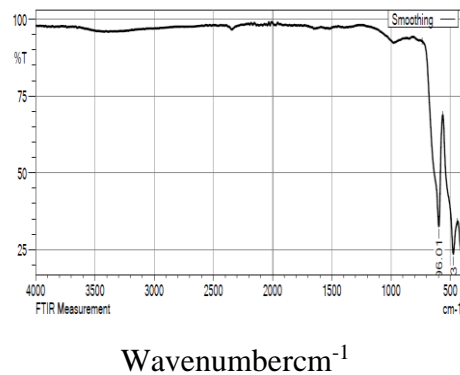
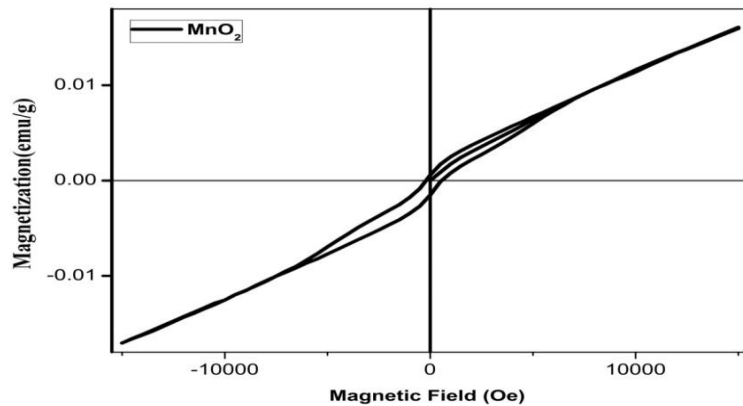


Fig 3.3 FTIR Spectrum of Mn₃O₄ nanoparticles

Magnetic behavior of MnO₂

Figure 1 depicts the M-H curve of MnO₂ nanoparticles at room temperature. It exposes the behaviour of ferromagnetic and antiferromagnetic materials. The measured M-H curve of MnO₂ indicates that magnetization in the low field area tends to saturate, but magnetization in the high field zone clearly displays unsaturated open linearity. This finding shows that the ferromagnetic component follows the Langevin pattern, but the antiferromagnetic component has a linear dependency.



CONCLUSION

In present study, The XRD patterns exposed the particles exhibit a pure structure of cubic. Simple chemical method has been used to successfully prepare Mn₂O nanoparticles, which are indexed as tetragonal Pyrolusite. The nanoparticles were estimated to be between 20 and 30 nm in

size. Analysis of functional group obtained from FT-IR exposed the stretching vibrations of metal ions in tetrahedral and octahedral co-ordination confirming the structure of crystal. The Antiferromagnetic behavior is detected at room temperature with no saturation magnetization and hysteresis in the area of measured field strength. These measurements as a function of temperature and field strength displayed a decrease in Antiferromagnetic temperatures.

References

1. Bhushan, B “Handbook of Nanotechnology”, publisher Springer, 1-5 (2010).
2. Wang, J., M. Lin, Y. Yan, Z. Wang, P.C. Ho, K.P. Loh, “CdSe/AsS Core-Shell Quantum Dots: Preparation and Two-Photon Fluorescence,” J. Am. Chem. Soc., 131, 11300-11301, (2009).
3. Kim, Y.T., J.H. Han, B.H. Hong, Y.U. Kwon, “Electrochemical synthesis of Cd-Se quantum-dot arrays on Graphene basal plane using mesoporous silica thin-film templates,” Adv. Mater., 22, 515-518, (2010).
4. Wang, Y., Q.Z. Qin, “A Nanocrystalline NiO Thin-Film Electrode Prepared by Pulsed Laser Ablation for Li-Ion Batteries,” J. Electrochem. Soc. 149(7), A873-A87, (2002).
5. Compagnini, G., A.A. Scalisi, O. Puglisi, “Production of gold nanoparticles by laser ablation in liquid alkanes,” J. Appl. Phys. 94, 7874-7877, (2003).
6. Dahl, J.A., B.L.S. Maddux, J.E. Hutchison, “Toward Greener Nano synthesis”, Chem. Rev. 107, 2228-2269, (2007).
7. Shah, M.A., T. Ahmad, “Principles of Nanoscience and Nanotechnology”, Narosa Publishing House, 32-65, (2010).
8. Jadhav, A.P., C.W. Kim, H.G. Cha, A.U. Pawar, N.A. Jadhav, U. Pal, Y.S. Kang, “Effect of Different Surfactants on the Size Control and Optical Properties of Y₂O₃:Eu³⁺ Nanoparticles Prepared by Coprecipitation Method,” J. Phys. Chem. C. 113, 13600–13604 (2009).
9. Kim, Y.T., J.H. Han, B.H. Hong, Y.U. Kwon, “Electrochemical synthesis of Cd-Se quantum-dot arrays on Graphene basal plane using mesoporous silica thin-film templates,” Adv. Mater., 22, 515-518, (2010).
10. Hankache, J. & Wenger, O.S. “Organic Mixed Valence”, Chem. Rev. 111, 5138-5178 (2011).
11. Young, C.G., (1989) “Mixed-valence compounds of the early transition-metals” *Coordination Chemistry Reviews.*, 96, 89-251.

12. Varma, C.M “Mixed-valence compounds”,*Reviews of Modern Physics.*, 48, 219-238., **(1976)**.
13. L.E. Foster, “Nanotechnology”, Personal Education, New Delhi, (2006) 143-145.
14. L. Ren, Y.P. Zeng, D. Jiang, *Solid State Sci.* 12, 138–143., **(2010)**.
15. G.Q. Zhang, N. Chang, D.Q. Han, A.Q. Zhou, X.H. Xu, *Mater. Lett.* 64, 2135–2137.,**(2010)**.
16. Latha Kumari, W.Z. Li, Charles H. Vannoy, Roger M. Leblanc, D.Z. Wang, *Ceram. Int.* 35, 3355–3364.,**(2009)**.
17. T. Selvamani, T. Yagy, S. Kawasaki, I. Mukhopadhyay, *Catal. Commun.* 11(2010) 537–541
18. S.M. Borghei, S. Kamali, M.H. Shakib, A. Bazrafshan, M.J. Ghoranneviss, *J. Fusion Energy* 30, 433–436.,**(2011)**.
19. J. Liu, L. Meng, Z. Fei, P.J. Dyson, X. Jing, X. Liu, MnO₂ nanosheets as an artificial enzyme to mimic oxidase for rapid and sensitive detection of glutathione. *Biosens. Bioelectron.* 90, 69 (2017)
20. Y. Zhang, Y. Li, C. Zhang, Q. Zhang, X. Huang, M. Yang, S.A. Shahzad, K.K.W. Lo, C. Yu, S. Jiang, Fluorescence turnon detection of alkaline phosphatase activity based on controlled release of PEI-capped Cu nanoclusters from MnO₂ nanosheets. *Anal. Bioanal. Chem.* 409, 4771 (2017)